Time-resolved buildup of twisted indirect exchange interaction in two-dimensional systems

V. A. Stephanovich,[1,*] E. V. Kirichenko,[1] V. K. Dugaev,[2] J. Barnaś,[3] and J. Berakdar[4]
[1]*Institute of Physics, Opole University, Opole 45-052, Poland*
[2]*Department of Physics and Medical Engineering, Rzeszów University of Technology, al. Powstańców Warszawy 6, 35-959 Rzeszów, Poland*
[3]*Faculty of Physics, Adam Mickiewicz University, ul. Umultowska 85, 61-614 Poznań, Poland*
[4]*Institut für Physik, Martin-Luther-Universität Halle-Wittenberg, Karl-Freiherr-von-Fritsch-Strasse 3, 06120 Halle (Saale), Germany*

(Received 2 April 2019; revised manuscript received 31 May 2019; published 17 June 2019)

We study theoretically the time-domain dynamics of the spin-dependent Ruderman-Kittel-Kasuya-Yosida (RKKY) interaction between driven magnetic impurities localized in a spin-orbit-coupled two-dimensional system. Particular attention is given to the influence of the spin-orbit coupling (SOC) on the system's dynamical response to a time-dependent precessional motion of the localized magnetic moment. We show that, via the RKKY mechanism, a flip of the spin z component of one localized moment affects all x, y, and z spin components of the other localized moment. The Friedel oscillations and the transient spin current triggered by the time-varying localized spin depend strongly on the orientation of the spin with respect to the two-dimensional structure. Our results demonstrate how the dynamic interplay between SOC and the RKKY interaction can be used to manipulate and fine-tune the characteristics of impurity spin reversal and to control the generated spin current and the local magnetization.

DOI: 10.1103/PhysRevB.99.235302

I. INTRODUCTION

A two-dimensional (2D) gas of nearly independent electrons (2DEG) with parabolic dispersion is formed when interfacing semiconductors or oxides materials. The 2D surface-confined state is also an inherent feature of the (111) surface of noble metals such as Cu(111). Such nonmagnetic noble metal surface states may turn spin-polarized when the surface is decorated by magnetic (for instance Co) adatoms and/or nanoislands, exhibiting new interference-driven features due to quantum confinement [1–3]. Generally, interference between incident and reflected waves results in spatially varying standing waves around scattering centers in the 2DEG. These standing waves are known as the energy-resolved Friedel oscillations and result in modulations in the local density of states around the defect, which can be mapped, for instance, by a scanning tunneling microscope (STM). While the wave nature of the 2DEG is essential in this regard, the surface imperfections can be completely classical, such as step edges, adsorbates [4], defects [5], or adatoms with large local magnetic moment, which can be placed deliberately using a spin-polarized STM, for example [6,7].

The electron density modulations around the adatom mediate a long-range oscillatory Friedel-type interaction with another adatom [8–11]. If the adatoms are magnetic, this stationary indirect [Ruderman-Kittel-Kasuya-Yosida (RKKY) [12]] interaction is spin-sensitive and couples magnetic moments ferromagnetically or antiferromagnetically, depending on their distance (see, e.g., [13,14], and references therein). Originally the RKKY interaction was treated in the frequency domain. Apart from this, the spin-orbit coupling (SOC), for instance of the Rashba type, is not essential for the appearance of the RKKY interaction. With the advent of time-dependent THz pulses [15,16] acting locally on the magnetization, and of the laser-induced magnetic (subpicosecond) switching [17], the question arose of how the spin-polarized charge-density accumulation builds up and eventually leads in the long-time limit to the well-established RKKY coupling. Furthermore, in the presence of SOC it is clear that the transient charge currents are also accompanied by transient spin currents, i.e., a flow of spin angular momentum. Such currents have been shown to be essential elements in spintronics and THz emitting devices based on nonequilibrium spin currents [18]. It is thus of interest to address the time-resolved RKKY mechanism in the presence of SOC.

Another aspect is that SOC can cause chaos in 2D confined systems [19,20]. This chaos (to be specific, chaotic trajectories of itinerant electrons in an exciton in 2DEG) can adversely influence the above dynamical manipulation of the spin states of magnetic impurities. This becomes especially important as normally the RKKY interaction becomes twisted due to SOC [21], which may completely disrupt the controlled manipulation of the impurity spin (and thus the corresponding device functionality) in case of chaos emergence.

How can we access the time-dependent, transient dynamics of the RKKY interaction? Obviously, a controlled time-dependent driving of one adatom is needed (as illustrated in Fig. 1) while monitoring in time observables that are sensitive to this adatom dynamics, such as the magnetization of a nearby adatom, time-evolution of the local spin-dependent charge density around the adatoms, or a possibly triggered spin current. One can envision a number of scenarios for realizing the time-dependent driving. For instance, the magnetic moment direction of a single 3D adsorbed adatom (Cr, Mn, Fe, and Co) can be controllably varied by changing the

*stef@uni.opole.pl

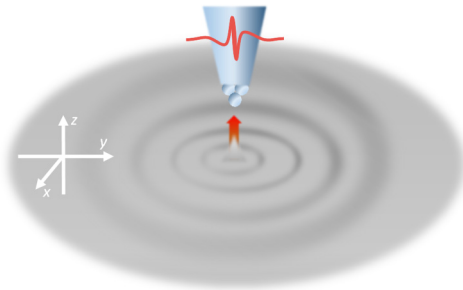

FIG. 1. A schematics of a possible realization of pumping the RKKY interaction via time variations of the local spin moment. A scanning tip acts locally on the magnetic moment leading to a transversal local spin dynamics. The time resolution may be achieved for instance by voltage bias pulses or THz pulses. We study then the buildup of the spin-resolved indirect exchange interaction.

distance between the adatom and the STM tip [22], which is, however, challenging to accomplish on the nano- or picosecond time scale.

Pulsed electromagnetic fields acting either on the tip or (directly on indirectly) on the localized moment enable ultrafast temporal resolution [23]. Indeed, in addition to optical fields, intense THz fields [15,16] combined with electron optics were realized to temporally control the tip-substrate interaction. On the nanosecond timescale, spin-polarized STM experiments were realized [24] using voltage pulses to achieve the time resolution. Pushing the time resolution to the ps time scale using voltage pulses is a challenge, however [25]. Here we focus on magnetic adatoms (or island), specifically on local spin excitations. We will not study how the local spin dynamics is triggered by the tip. This has been done in numerous previous works (see, for instance, Ref. [25] and references therein). The problem addressed in this work is how the spin-dependent response of the electronic surrounding builds up upon time-varying local magnetic moments. A schematic of a possible experimental realization is depicted in Fig. 1.

It is obvious now that a key ingredient in the phenomena discussed below is the spin-orbital coupling active in the 2DEG. This has important consequences for ultrafast (subpicosecond) spin-dependent dynamics, as is known from other problems involving SOC-related effects [17,26–42]. In the context of the present work, it is known that a Rashba-type SOC in the 2DEG twists the ordinary RKKY interaction in 1D and 2D systems [21]. Thus, we expect the generation of spin current once the magnetization of the local impurities is fluctuating. From the established meaning of the RKKY interaction, and in fact from the way it is calculated below, it is clear that this spin current is related to the spin-resolved nature of the particle-hole excitations in the 2DEG, which is principally different from the magnonic spin current [43], which occurs, for instance, in magnetic insulators and can be captured by classical methods (if quantum fluctuations are suppressed) such as the Landau-Lifshitz equation; also the time and energy scales of both types of spin currents are different, as follows from the results below. Our findings evidence that in contrast to the case without SOC [44], both the emergent dynamic spin polarization and spin current are highly anisotropic. Specifically, we study here the influence of SOC on the response to fast processional reversal of a single impurity spin $\mathbf{S}_0(t)$, which is coupled to the host 2DEG by (s-d) exchange interaction. The magnetic polarization of the 2DEG is manifested as time-dependent Friedel oscillations that are dependent on the SOC constant γ and are highly anisotropic. A flip of one spin component (say S_z) induces a dynamics in all three spin components. This means, in turn, that all nine components of the spin response tensor S_{mn} ($m, n = x, y, z$), quantifying the response of the mth spin component to flip of the nth one, may become finite.

II. PROPAGATING SPIN-DENSITY OSCILLATIONS

A localized magnetic impurity (s-d) coupled to the itinerant carriers of the 2DEG is captured by the following Hamiltonian:

$$\mathcal{H} = -\frac{\hbar^2\Delta}{2m} - i\gamma\,(\sigma_x\nabla_y - \sigma_y\nabla_x) + \frac{g}{n}\,\boldsymbol{\sigma}\cdot\mathbf{S}_0(t), \qquad (1)$$

where the first term represents the usual kinetic energy (Δ is a 2D Laplace operator, m is an electron effective mass), while the second term describes the Rashba SOC with the coupling strength γ. The last term stands for the exchange coupling between the local spin and 2DEG. Here, $n = N/A$ is the sheet density of host atoms (A is the area of 2DEG), g is the local s-d coupling constant, $\boldsymbol{\sigma}$ stands for the vector of Pauli matrices, and $\mathbf{S}_0(t)$ is the dynamic spin of the magnetic impurity, which is assumed to be large enough so that it can be treated classically. The exchange interaction between the itinerant electrons and localized spin $\mathbf{S}_0(t)$ generates the Friedel oscillations in the electron spin density $\mathbf{s}(\mathbf{r}, t)$, which appear around the localized spin (cf. Fig. 1).

In general, g is quite small compared with the Fermi energy and hence we may obtain a reliable expression for the response of 2DEG to the impurity spin flip using the perturbation theory with respect to the coupling constant g [12]. To do this, we construct first the unperturbed (i.e., for $g = 0$) Green's function of the problem on the base of the spectrum of the unperturbed version of Hamiltonian (1),

$$E^{\mu}_{\mathbf{k}} = \frac{\hbar^2k^2}{2m} \pm \hbar\gamma k \equiv \frac{\hbar^2k^2}{2m} + \mu\hbar\gamma k, \qquad (2)$$

where $\mu = \pm 1$ is the chirality index [45–47], which defines two subbands of the electron energy spectrum (2). In turn, the eigenvectors of the unperturbed Hamiltonian have the form

$$\Psi_{\mu}(\mathbf{r}) = \frac{e^{i\mathbf{k}\cdot\mathbf{r}}}{\sqrt{2A}}\begin{pmatrix} ie^{-i\varphi} \\ \mu \end{pmatrix}, \quad \varphi = \arctan\frac{k_y}{k_x} \qquad (3)$$

and we define the unperturbed Green's function as follows [48]:

$$G_0(\mathbf{r}, \mathbf{r}', t) = \sum_{k,\mu=\pm1} \Psi_{\mathbf{k}\mu}(\mathbf{r})\,\Psi^{\dagger}_{\mathbf{k}\mu}(\mathbf{r}')\,e^{-it(E^{\mu}_{\mathbf{k}}-E_F)/\hbar}, \qquad (4)$$

where E_F is the Fermi energy. Note that the Green's function (4) has a matrix form [21,45]. We have explicitly

$$\sum_k \Psi_{\mathbf{k}\mu}(\mathbf{r})\Psi^{\dagger}_{\mathbf{k}\mu}(\mathbf{r}') = \frac{1}{2A}\int_0^{\infty} k\,dk \int_0^{2\pi} d\varphi\, e^{i\mathbf{k}(\mathbf{r}-\mathbf{r}')}\begin{pmatrix} 1 & i\mu e^{-i\varphi} \\ -i\mu e^{i\varphi} & 1 \end{pmatrix}. \qquad (5)$$

When performing the angular integration, we took into account that the angle $\alpha = \arctan[(y-y')/(x-x')]$ enters the definition of the Bessel function $J_1(\eta)$ ($\eta = k|\mathbf{r}-\mathbf{r}'|$) [49],

$$\int_0^{2\pi} d\varphi\, e^{i\mathbf{k}(\mathbf{r}-\mathbf{r}')}\, e^{\pm i\varphi} = 2\pi i e^{\pm i\alpha} J_1(\eta).$$

This angular dependence of the Green's function stems from the presence of SOC, and this dependence is a source of all subsequent twists and anisotropies of the exchange interaction as modified by SOC. The anisotropy of the spin density and spin current distribution related to the dependence on the angle α is a peculiarity of Friedel oscillations, which arises due to SOC that couples the spatial motion of an electron to its spin.

Upon calculating the angular integrals, one finds the following final expressions for the unperturbed Green's function:

$$G_{0\mu}(\mathbf{r},\mathbf{r}',t,t') = -\frac{i}{4\pi A}\int_{k_\mu}^{\infty} k\,dk\; e^{-i(t-t')[\frac{E^\mu_{\mathbf{k}}-E_F}{\hbar}-i\Gamma]} \times \begin{pmatrix} J_0(\eta) & -\mu J_1(\eta)e^{-i\alpha} \\ \mu J_1(\eta)e^{i\alpha} & J_0(\eta)\end{pmatrix}, \quad t-t'>0,\ k>k_\mu, \tag{6}$$

$$G_{0\mu}(\mathbf{r},\mathbf{r}',t,t') = \frac{i}{4\pi A}\int_{0}^{k_\mu} k\,dk\; e^{-i(t-t')[\frac{E^\mu_{\mathbf{k}}-E_F}{\hbar}+i\Gamma]} \times \begin{pmatrix} J_0(\eta) & -\mu J_1(\eta)e^{-i\alpha} \\ \mu J_1(\eta)e^{i\alpha} & J_0(\eta)\end{pmatrix}, \quad t-t'<0,\ k<k_\mu, \tag{7}$$

where $J_{0,1}(z)$ are the Bessel functions [49]. Here, k_μ is defined by the condition $E^\mu_{\mathbf{k}}(k_\mu) = E_F$, or equivalently $k_\mu = k_F - \mu k_R$, where $k_F = \pm\sqrt{k_{F0}^2 + k_R^2}$ is the SOC-modified Fermi momentum. In turn, $k_{F0} \equiv (2mE_F)^{1/2}/\hbar$ is the bare (without SOC) Fermi momentum and $k_R = m\gamma/\hbar^2$ is the Rashba one. Also, $E^\mu_{\mathbf{k}}$ is given by Eq. (2) and $\Gamma = \hbar/2\tau$ is the electron relaxation rate (the momentum relaxation time τ) related to electron scattering on impurities and/or other structural defects. Note that for convenience in the subsequent calculations, where the summation over chiralities is to be made explicitly, we do not sum over the chirality index μ and thus we obtain the expressions for partial (for each μ) Green's functions.

In the lowest order of perturbation theory, the spatial and temporal dependence of a response $\mathbf{R}(\mathbf{r},t)$ of the electron spin to the time-dependent flip of the dynamic magnetic impurity $\mathbf{S}_0(t)$ can be written in the following form [48]:

$$R_m(\mathbf{r},t) = -\frac{ig}{\hbar}\sum_{\mu,\nu=\pm1}\sum_{n=x,y,z}\mathrm{Tr}\int_{-\infty}^{t} S_{mn\mu\nu}(\mathbf{r},t,t')dt',$$

$$S_{mn\mu\nu}(\mathbf{r},t,t') = \sigma_m G_{0\mu}(\mathbf{r},t,0,t') \times \sigma_n S_{0n}(t')\, G_{0\nu}(0,t',\mathbf{r},t'). \tag{8}$$

Here $m,n = x,y,z$; μ,ν describe the chiralities, and Tr stands for the trace over spin indices. Here we introduce *the spin-response tensor* $S_{mn\mu\nu} \equiv S_{mn}$ $(m,n=x,y,z)$, which gives the response of the mth spin component to the flip of the nth one. This tensor structure actually reflects the twisting of the spin density (and thus also of the RKKY coupling) in the presence of SOC. To obtain the mth component of spin response function (8), one has to sum over all three components $\sigma_n S_{0n}(t')$ in the spin-response tensor.

Substitution of Eqs. (6) and (7) into Eq. (8) gives the magnetic response of 2DEG to the time-dependent perturbation $S_{0\mu}(t)$. For arbitrary $m,n = x,y,z$, evaluation of the corresponding traces over the spin indices (being in this case a cumbersome task due to the matrix structure of Green's function) generates the above spin-response tensor. In the experimental setups for RKKY interaction pumping, each of the components S_{mn} can appear depending of the problem geometry and tip scanning directions.

The experimental setup discussed here consists of a spin-polarized scanning tip placed on top of the 2D structure (say, a metal or semiconductor layer). The tip is assumed to act effectively on the localized magnetic moment with a magnetic field $\mathbf{B}$ oriented perpendicularly to the surface. This field tends to align the spin direction of the localized magnetic impurity $\mathbf{S_0}$ with that of the tip. This triggers a Larmor precession of $\mathbf{S_0}$ in the magnetic field $\mathbf{B}$, which is usually described by the Bloch equations [50]. If the STM magnetization is switched back and forth along the z axis, this would trigger the dynamics of the localized impurity spin in x and y directions. For simplicity (and without limitation of generality), here we choose for $\mathbf{S_0}$ a uniform dynamics along the y axis only, which implies

$$S_{0y}(t) = \begin{cases} \tilde{S}_0\cos(\pi t/T), & |t| < T/2, \\ 0, & |t| \geqslant T/2, \end{cases} \tag{9}$$

where T is the spin-flip time. Using Eq. (8) as well as Eqs. (6) and (7), upon calculating the traces, we finally obtain the following expression for the y component of spin response:

$$\begin{aligned} R_y(\mathbf{r},t) = -\frac{ig}{4\pi^2\hbar}\sum_{\mu,\nu=\pm1}\int_{-\infty}^{t} S_{0y}(t')dt' \\ \times\Bigg\{\int_{k_\mu}^{\infty} e^{i\frac{t-t'}{\hbar}(E^\mu_{\mathbf{k}}-E^\nu_{\mathbf{k}_1}-2i\Gamma)} k\,dk\int_0^{k_\nu}[J_0(kr)J_0(k_1r) \\ -\mu\nu\cos2\alpha J_1(kr)J_1(k_1r)]k_1dk_1 \\ -\int_{k_\nu}^{\infty} e^{i\frac{t-t'}{\hbar}(E^\mu_{\mathbf{k}}-E^\nu_{\mathbf{k}_1}-2i\Gamma)} k_1dk_1\int_0^{k_\mu}[J_0(kr)J_0(k_1r) \\ -\mu\nu\cos2\alpha J_1(kr)J_1(k_1r)]k\,dk\Bigg\}. \end{aligned} \tag{10}$$

For very long spin-flip time, $T\to\infty$ (more exactly, if the spin-flip time T is longer than the electron relaxation time τ so that $\tau\to\infty$ or $\Gamma\to0$), the expression (10) yields a time-independent function, which can be approximated by the ordinary 2D static RKKY function [51–53] but with a SOC-modified Fermi momentum,

$$R_y(\mathbf{r}) \simeq -\frac{gmk_F^2\tilde{S}_0}{8\pi n^2\hbar^2}[J_0(q)N_0(q)+J_1(q)N_1(q)], \quad q = k_Fr \equiv r\sqrt{k_{F0}^2+k_R^2}, \tag{11}$$

where $N_0(q)$ and $N_1(q)$ are the Neumann functions [49]. In Eq. (11), this approximation works well for $\kappa_R^2 < 1/3$ ($\kappa_R = k_R/k_{F0}$); see Ref. [45] for details.

Other components of the spin response tensor S_{mn} can also be calculated. Denoting the *bare* (i.e., those without time-dependent exponentials) integrands of the corresponding components as Q_{mn}, we obtain

$$\begin{aligned} Q_{xx} &= 2(Q_0 + \mu\nu Q_1 \cos 2\alpha), \\ Q_{yy} &= 2(Q_0 - \mu\nu Q_1 \cos 2\alpha), \\ Q_{zz} &= 2(Q_0 + \mu\nu Q_1), \\ Q_{xy} &= 2Q_1 \sin 2\alpha, \ Q_{xz} = Q_2 \cos\alpha, \ Q_{yz} = Q_2 \sin\alpha. \\ Q_0 &= J_0(kr)J_0(k_1 r), \ Q_1 = J_1(kr)J_1(k_1 r), \\ Q_2 &= 2(\mu + \nu)[J_0(k_1 r)J_1(kr) - J_0(kr)J_1(k_1 r)]. \end{aligned} \tag{12}$$

Here $Q_{xy} = Q_{yx}$, while $Q_{xz} = -Q_{zx}$ and $Q_{yz} = -Q_{zy}$, reflecting the twisted structure of the RKKY interaction in the presence of SOC. We note here that the spin-response tensor components differ from those of the spin susceptibility tensor, introduced, for instance, in Ref. [54] (see also Ref. [55], where the anisotropic RKKY coupling constants, due to the Dirac surface electronic states, have been calculated). This is because our impurity spin $\mathbf{S}_0(t)$ is reorientable so that all time instants of its reorientation make a contribution to the integral (8) over the second time variable t'. Our aim is to calculate the *time-resolved* (i.e., transient) characteristics of the electron response to a flip of the localized magnetic impurity. In our case it is more convenient not to separate the contributions from XY, Heisenberg, and/or Dzyaloshinskii-Moriya interactions into our dynamics. We focus on the joint action of RKKY time-dependent twisting (which actually mixes the aforementioned contributions) in the 2DEG response. That is why we calculate the time-dependent 2DEG spin-density oscillations as well as those of spin current, as discussed below.

Note that while in the absence of SOC [44] only the diagonal components of S_{mn} are nonzero, now all nine components can be finite. This is simply because now the spin structure of the Green's function (6) and (7) becomes much more complex so that traces over spin indices render possible finite values of all nine S_{mn} tensor components. Our calculations show that the spatial and temporal dependencies of all S_{mn} components are qualitatively similar to each other, although the static limit for off-diagonal components $m \neq n$ differs from the standard 2D RKKY function (11). We calculated the components (10) in detail, while other components (12) can be calculated if needed for a specific experimental situation.

To calculate the component R_y (10) numerically, we render it in the form R_y/R_{y0} and introduce the following dimensionless variables: $R_{y0} = gk_F^4\tilde{S}_0/(4\pi^2\varepsilon_F n^2)$, $t_0 = \varepsilon_F t/\hbar$, $\tau_0 = \varepsilon_F \tau/\hbar$, and $T_0 = \varepsilon_F T/\hbar$. The influence of the Rashba parameter κ_R and the angle α on the spatial dependence of the oscillating spin density is shown in Fig. 2. Panel (a) shows the dependence on the dimensionless SOC constant κ_R. It can be seen that this dependence is not very strong so that the curves for $\kappa_R = 0$ and 0.1 almost coincide (on the scale of the plots). The spatial angular dependence of the oscillating spin density, which is presented in Fig. 2(b),

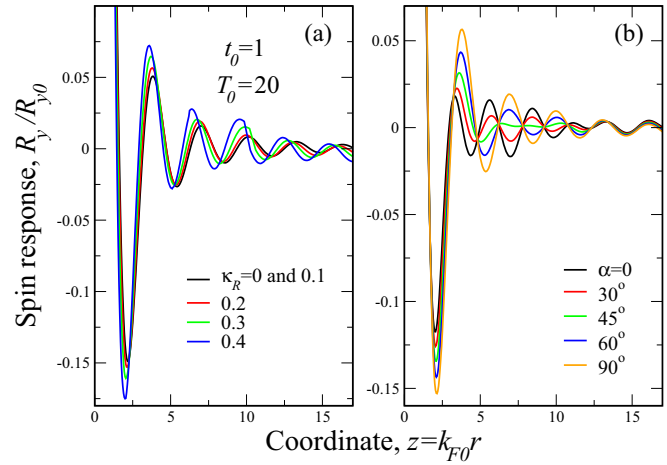

FIG. 2. Spin-density oscillations for the dimensionless time $t_0 = 1$, spin-flip time $T_0 = 20$, and relaxation time $\tau_0 = 100$. Panel (a) shows the dependence on the dimensionless Rashba constant κ_R, as indicated in the legend. Panel (b) shows the dependence on the anisotropy angle α as listed in the legend. The curves in panel (b) correspond to $\kappa_R = 0.3$.

has been plotted for $\kappa_R = 0.3$. The plots for other values of κ_R are qualitatively similar. The choice of the angular range, $0 < \alpha < 90^\circ$, is dictated by the character of angular dependence in Eq. (10), i.e., by the factor $\cos(2\alpha)$, which is π-periodic. This means that the range $0 < \alpha < 90^\circ$ (half period) covers all possible cases. The angular dependence (i.e., the anisotropy) of the dynamic spin density is stronger than that on κ_R. The maximal amplitude of the spin-density oscillations for the chosen $t_0 = 1$ and $T_0 = 20$ occurs for $\alpha = 90^\circ$. At large $z = k_{F0}r \sim 10$–15, the anisotropy vanishes and the curves for different α merge into a single one. This shows that the influence of SOC disappears at large distances from the localized spin S_0. A similar effect has been obtained in the work [19], where SOC was the reason for chaotization of the relative electron and hole motion in an exciton, which naturally has a finite spatial extension. It can be shown that for $\kappa_R = 0$, all terms containing α in Eq. (10) cancel mutually and the system becomes isotropic [44].

Figures 3(a)–3(c) show the spatial spin density oscillations for different values of t_0 and for the indicated value of T_0. The static case (11) is also presented there by the broken line. The curves in panels (a)-(c) correspond to $\kappa_R = 0.3$—the curves for other values of $0 < \kappa_R < 0.4$ are qualitatively similar. Also, the dependence for $\alpha \neq 90^\circ$ is qualitatively similar to that shown in the panels (a)–(c). We have chosen the case $\alpha = 90^\circ$, as the curves are then well distinguishable on the scale of the plot. One can see from Figs. 3(a)–3(c) that at large spin-flip times $T_0 = 20$ and small running times $t_0 = 1$, the system is closer to the static case than in the opposite situation of small T_0 and large t_0. This behavior is due to the interplay between SOC and the retardation of the system time response to the localized spin flip (9), which *spoils* the regular Friedel oscillations given by Eq. (11), meaning that the period and decay rate of the ordinary Friedel oscillations are modified by the interplay of SOC and the RKKY interaction. The period and the decay rate of the Friedel oscillations had

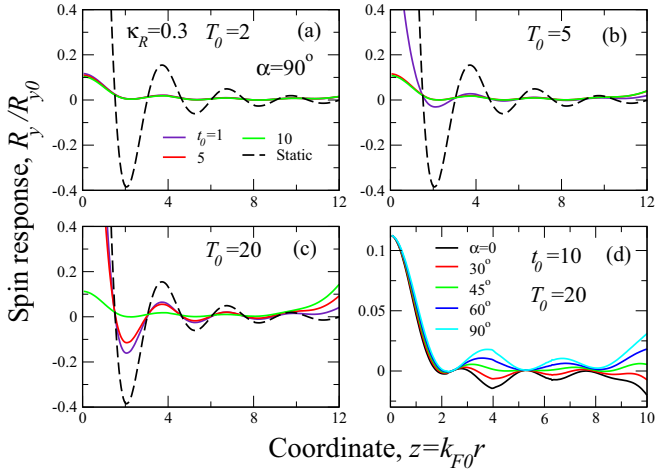

FIG. 3. Same as in Fig. 2 for different values of t_0 [see the legend in (a)]. Parts (a)–(c) correspond to different values of T_0 as shown in each panel. The static case (11) is shown by the broken line in (a)–(c). Dimensionless parameters: $\tau_0 = 100$, $\kappa_R = 0.3$. (a)–(c) $\alpha = 90^\circ$ [shown in (a)]; (d) the α-dependence for the parameters indicated in the panel.

been discussed in Ref. [56], as well as in Ref. [57] in the context of the dynamic RKKY interaction in graphene (hence no SOC). Note that the graphene-based structures can be used in novel magnetic memory devices [58]. It is possible that some chaotic features, which may arise in the system with SOC (see above), may be responsible for these distortions; see also the irregular behavior in Figs. 4–6 below.

Panel (d) in Fig. 3 shows the spin-density angular dependence at typical experimentally relevant values; $t_0 = 10$ and $T_0 = 20$. This choice of parameters has been dictated by the experimental situation in femtosecond optical switching: 80 fs [59], and 60 and 12 fs [40]. The shortest pulse duration corresponds to $T_0 = 20$ ($\varepsilon_F = 1$ eV) or $T_0 = 2$ ($\varepsilon_F = 0.1$ eV).

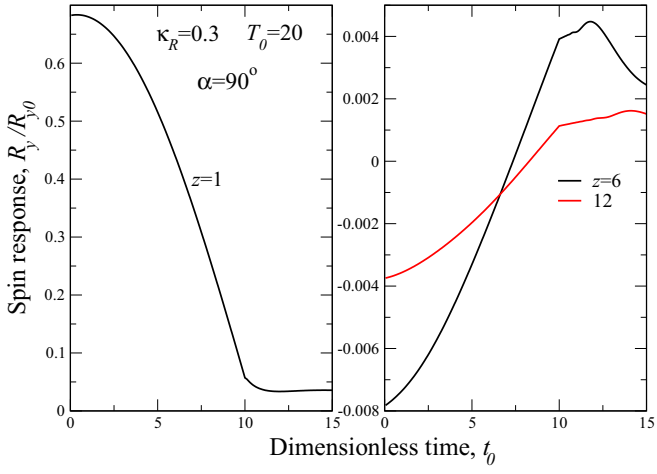

FIG. 4. Spin-density Friedel oscillations at different spatial points z (legends in the panels). The left panel reports the time dependence at $z = 1$, where the corresponding values of spin density are around 100 times larger than those for $z = 6$ and 12 (right panel). Dimensionless parameters: $\kappa_R = 0.3$, $T_0 = 20$, and $\tau_0 = 100$.

Electron momentum relaxation time is in the picosecond range, so that everywhere we use $\tau_0 = 100$.

The temporal evolution of the spin density is shown in Fig. 4. The amplitude of the system response is 100 times smaller at $z = k_{F0}r = 6$ and 12—details of the corresponding curves are reported in the right panel. The main effect here (apart from very fast decay at growing z) is the time lag in the system response as the distance from the magnetic impurity spin grows. Indeed, while at $z = 1$ the maximal response occurs at $t_0 \approx 1$, at larger distances the maximal response (although it is much smaller than that at $z = 1$) occurs at $t_0 \approx 10$. This demonstrates the retardation effect, when the system response appears earlier at small distances from the impurity spin.

III. SPIN CURRENT AND ITS ANISOTROPY

Now we shall calculate the spin current emitted by a time-dependent local spin moment. In contrast to the case without SOC [44], the tensor structure of spin current becomes more complex, having more finite components. Similarly to the case of a spin-response tensor, S_{mn}, all spin current components behave in a qualitatively similar manner. That is why we discuss only one component, keeping in mind that each additional component can be evaluated along the lines of the present study.

For the system under consideration, the spin-current operator can be written as

$$\hat{J}_i^m = \frac{i\hbar}{2m}\,(\overleftarrow{\nabla}_i - \overrightarrow{\nabla}_i)\,\sigma_m, \tag{13}$$

where the index i ($i = x, y$) defines the ordinary 2D coordinate in the x-y plane, while the index m ($m = x, y, z$) defines the spin current projection. In turn, the arrows over the operator ∇_i indicate the direction of the operator action.

Within the approach used in this paper, the expectation value of the spin current can be written in the following form:

$$J_i^m(\mathbf{r}, t) = -\frac{g}{2m}\sum_{\mu,\nu=\pm1}\mathrm{Tr}\int_{-\infty}^{t} S_{0n}(t')dt'\left[\frac{\partial}{\partial r_i} - \frac{\partial}{\partial r_i'}\right] \times \sigma_m\, G_{0\mu}(\mathbf{r}, t, 0, t')\,\sigma_n G_{0\nu}(0, t', \mathbf{r}', t)|_{\mathbf{r}=\mathbf{r}'}. \tag{14}$$

It is worth noting that the main difference, when compared to the case without SOC, is that now we have to differentiate with respect to $r_i = x, y$ because of the phase factors $e^{\pm i\alpha}$; see Eqs. (6) and (7). Then, the spin current components cannot be expressed through a single quantity, i.e., through the radial current $J^m(\mathbf{r}, t)$. This means that now, similarly to the case considered above of spin response tensor S_{mn}, the spin current also acquires an explicit tensor form, which is an additional manifestation of the twisting of the RKKY interaction. We emphasize that this twisted form is a consequence of the Rashba-type spin-orbit interaction in the 2DEG.

As in the case of spin density, calculation of a general tensor structure of the spin current becomes rather tedious. For the experimentally relevant case, as, for instance, in Eq. (9), we calculate the spin current component $J_x^y(\mathbf{r}, t)$. The

corresponding explicit expression for this component reads

$$J_x^y(\mathbf{r},t) = \frac{g}{8m\pi^2A^2}\sum_{\mu,\nu=\pm1}\int_{-\infty}^{t} S_{0y}(t')\,dt' \times\Bigg\{\int_{k_\mu}^{\infty} e^{i\frac{t-t'}{\hbar}(E^\mu_{\mathbf{k}}-E^\nu_{\mathbf{k}_1}-2i\Gamma)}k^2dk\int_0^{k_\nu} f(k,k_1)k_1dk_1 - \int_{k_\mu}^{\infty} e^{i\frac{t-t'}{\hbar}(E^\mu_{\mathbf{k}}-E^\nu_{\mathbf{k}_1}-2i\Gamma)}k\,dk\int_0^{k_\nu} f(k,k_1)k_1^2dk_1 - \int_0^{k_\mu} e^{i\frac{t-t'}{\hbar}(E^\mu_{\mathbf{k}}-E^\nu_{\mathbf{k}_1}-2i\Gamma)}k^2dk\int_{k_\nu}^{\infty} f(k,k_1)k_1dk_1 + \int_0^{k_\mu} e^{i\frac{t-t'}{\hbar}(E^\mu_{\mathbf{k}}-E^\nu_{\mathbf{k}_1}-2i\Gamma)}k\,dk\int_{k_\nu}^{\infty} f(k,k_1)k_1^2dk_1\Bigg\}, \tag{15}$$

where we introduced the following notation:

$$f(k,k_1) = J_1(kr)J_0(k_1r) - J_0(kr)J_1(k_1r) + \frac{2\mu\nu}{kr}J_1(kr)J_1(k_1r)\sin^2\alpha\left(\frac{1}{kr}-\frac{1}{k_1r}\right) - \mu\nu(J_1(kr)J_Q(k_1r) - J_1(k_1r)J_Q(kr))\cos 2\alpha,$$
$$J_Q(p) = \frac{dJ_1(p)}{dp} = \frac{1}{2}[J_0(p) - J_2(p)]. \tag{16}$$

It can be shown that in the absence of SOC, when $\gamma = 0$ and the angle $\alpha = 0$, the tensor structure of the spin current (related to the twisting of the exchange interaction) disappears and one recovers the earlier results [44], where all spin current components could be expressed through the radial spin current. Our analysis also shows that in the static limit ($T \to \infty$, $\tau \to \infty$) each of the spin-current components presented above vanishes exactly. This situation is opposite to that with the dynamic spin density and reflects simply the fact that there is no spin flow in the thermodynamic equilibrium.

The spatial dependence of the spin-current component J_x^y [normalized by the quantity $J_0 = gk_{F0}^5\hbar\tilde{S}_0/(8\pi^2m\varepsilon_F n^2)$] is presented in Fig. 5 for different values of t_0 and T_0. Our analysis shows that the behavior of the other spin-current components is qualitatively similar to that reported in Fig. 5. Contrary to the case of spin density, where the most remarkable situation occurs for $\alpha = 90°$, we plot here the curves for $\alpha = 30°$. The angular dependence becomes substantial at the intermediate coordinates $1 < z < 8$, as can be seen in Fig. 5(d). Similarly to the case of the spin dynamics shown in Fig. 3, the physical picture here is determined by the interplay between the SOC constant γ (reflected both directly and via the angle α) and the time constants t_0 and T_0. Two irregular oscillations are clearly seen, which means that in the presence of SOC, the external spin-flip not only generates the spin current but also *spoils* the corresponding regular Friedel oscillations of the current. Apart from this, the nonmonotonic dependence on t_0 and T_0 can be observed in Fig. 5. Namely, depending on T_0, the curves for smaller t_0 can lie below those for larger t_0; see Figs. 5(a)–5(c). Note that SOC adds a slow decay of the spin current to the irregular character of the oscillations: The spin current starts to decay substantially

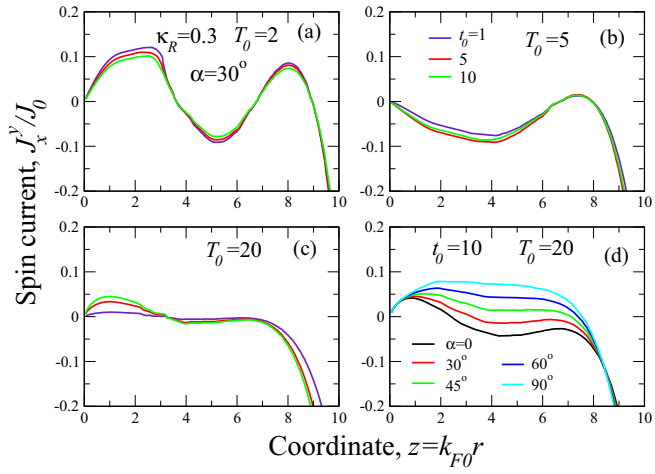

FIG. 5. Spatial oscillations of the spin-current component J_x^y at different values of t_0 [legend in (b)]. Panels (a)–(c) correspond to different T_0 as shown in each panel. Dimensionless parameters: $\tau_0 = 100$, $\kappa_R = 0.3$. (a)–(c) $\alpha = 30°$ [shown in (a)]. Panel (d) shows the α-dependence for the parameters as indicated.

(depending on component J_i^j) at $z > 20$–30. This is to be compared to the case of $\gamma = 0$ [44].

The temporal evolution of J_x^y is reported in Fig. 6. As the current amplitude is much larger at $z = 12$ (due to the slow spatial decay of J_x^y; see above), the corresponding details are shown separately in the right panel. In this case, the angular dependence is not very prominent so that we plot the curves for $\alpha = 30°$. Figure 6 illustrates the spin pumping, which is clearly seen in the left panel at $k_{F0}r = 1$, where the spin current rises in time while the pulse lasts (up to more or less $t_0 = 10$), and then sharply drops after the pulse ends. We recall here that the spin-flip time (related to the pulse duration) is chosen as $T_0 = 20$. A similar behavior (on a smaller scale and a different direction) occurs for $z = 6$. At the same time, for

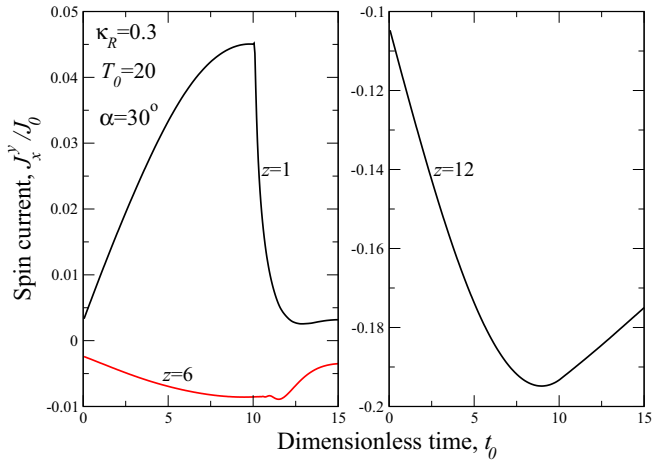

FIG. 6. Temporal evolution of the spin current J_x^y taken at different spatial points (indicated near the curves). The left panel shows the time dependence for $k_{F0r} = 1$ and 6, while the right panel (due to different scale) shows the case $z = 12$. The curves are plotted for $\kappa_R = 0.3$, $\alpha = 30°$, $T_0 = 20$, and $\tau_0 = 100$.

$z = 12$ (far from the source) the spin current does not grow at all due to retardation effects, and it starts to decay already at $t_0 = 0$.

IV. OUTLOOK

In this paper, we have analyzed the dynamical RKKY interaction in a 2DEG with Rashba spin-orbit interaction. We have demonstrated that the interplay of spin-orbit coupling of Rashba-type and RKKY interaction results in interesting dynamical phenomena, such as, for instance, strong anisotropy of the system response to a flip of a localized magnetic moment. The corresponding dynamic spin response and spin current acquire then a tensor structure with all components being generally nonzero, in contrast to the diagonal structure when the Rashba SOC is absent. Considering the spin-orbit and RKKY interactions in the time domain, we have determined the temporal evolution of the spin excitations and associated spin current due to a fast reversal of a localized spin. The presented formalism captures properly the basic features of this propagation. From the analysis, it also follows that the SOC in the 2DEG facilitates the spin relaxation upon an external excitation (reversal) of the localized magnetic moment. We note that such a very fast reversal of a localized spin may be achieved with local scanning techniques such as spin-polarized STM, as discussed in the Introduction.

The SOC-related chaotic internal motion in 2D confined systems [19,20] may substantially influence the fast manipulation of the localized magnetic impurities in 2D systems. It remains to be clarified whether the irregular oscillatory behavior in the spin density and spin current, induced by the interplay between spin-orbit and RKKY interactions, may be related to a precursor of possible chaotic behavior. An additional hint for this follows from the fact that the SOC-induced anisotropy spreads over a finite distance; see Fig. 2(b). One can easily imagine the situation when electron-hole interactions (such as the Coulomb interaction in an exciton) in 2DEG generate some bound states, which not only preclude fast magnetization switching but also may be prone to chaos. Therefore, despite the relativistic character of spin-orbit coupling, its interplay with (generally much stronger) indirect RKKY exchange interaction generates many interesting phenomena, which should be studied in the future, both experimentally and theoretically.

ACKNOWLEDGMENTS

This work was supported by the National Science Center in Poland as a research Project No. DEC-2017/27/B/ST3/02881 and by the DFG through SFB-TRR227.

[1] L. Diekhöner, M. A. Schneider, A. N. Baranov, V. S. Stepanyuk, P. Bruno, and K. Kern, Phys. Rev. Lett. **90**, 236801 (2003); O. Pietzsch, A. Kubetzka, M. Bode, and R. Wiesendanger, *ibid.* **92**, 057202 (2004); E. Y. Tsymbal, O. N. Mryasov, and P. R. LeClair, J. Phys.: Condens. Matter **15**, R109 (2003); W. Wulfhekel and J. Kirschner, Appl. Phys. Lett. **75**, 1944 (1999); R. Wiesendanger, M. Bode, and M. Getslaff, *ibid.* **75**, 124 (1999); S. Rusponi, N. Weiss, T. Cren, M. Epple, and H. Brune, *ibid.* **87**, 162514 (2005); J. A. Stroscio, D. T. Pierce, A. Davies, R. J. Celotta, and M. Weinert, Phys. Rev. Lett. **75**, 2960 (1995); M. Bode, M. Getzlaff, and R. Wiesendanger, *ibid.* **81**, 4256 (1998); S. N. Okuno, T. Kishi, and K. Tanaka, *ibid.* **88**, 066803 (2002); T. K. Yamada, M. M. J. Bischoff, G. M. M. Heijnen, T. Mizoguchi, and H. van Kempen, *ibid.* **90**, 056803 (2003); L. Niebergall, V. S. Stepanyuk, J. Berakdar, and P. Bruno, *ibid.* **96**, 127204 (2006).

[2] R. Wiesendanger, Rev. Mod. Phys. **81**, 1495 (2009).

[3] H. Oka, O. O. Brovko, M. Corbetta, V. S. Stepanyuk, D. Sander, and J. Kirschner, Rev. Mod. Phys. **86**, 1127 (2014).

[4] H. Brune, J. Wintterlin, G. Ertl, and R. J. Behm, Europhys. Lett. **13**, 123 (1990); M. F. Crommie, C. P. Lutz, and D. M. Eigler, Science **262**, 218 (1993); Ph. Avouris, I.-W. Lyo, R. E. Walkup, and Y. Hasegawa, J. Vac. Sci. Technol. B **12**, 1447 (1994).

[5] H. A. Mizes and J. S. Foster, Science **244**, 559 (1989); M. Schmid, W. Hebenstreit, P. Varga, and S. Crampin, Phys. Rev. Lett. **76**, 2298 (1996).

[6] J. Repp, F. Moresco, G. Meyer, K.-H. Rieder, P. Hyldgaard, and M. Persson, Phys. Rev. Lett. **85**, 2981 (2000).

[7] M. F. Crommie, J. Electron Spectrosc. Relat. Phenom. **109**, 1 (2000); S. Crampin and O. R. Bryant, Phys. Rev. B **54**, R17367 (1996).

[8] J. Friedel, Nuovo Cimento Suppl. **7**, 287 (1958).

[9] K. H. Lau and W. Kohn, Surf. Sci. **75**, 69 (1978).

[10] P. Hyldgaard and M. Persson, J. Phys.: Condens. Matter **12**, L13 (2000).

[11] V. S. Stepanyuk, A. N. Baranov, D. V. Tsivlin, W. Hergert, P. Bruno, N. Knorr, M. A. Schneider, and K. Kern, Phys. Rev. B **68**, 205410 (2003).

[12] M. A. Ruderman and C. Kittel, Phys. Rev. **96**, 99 (1954); T. Kasuya, Prog. Theor. Phys. **16**, 45 (1956); K. Yosida, Phys. Rev. **106**, 893 (1957); see also C. Kittel, *Quantum Theory of Solids* (Wiley, New York, 1987).

[13] Yu. G. Semenov and V. A. Stephanovich, Phys. Rev. B **66**, 075202 (2002).

[14] Yu. G. Semenov and V. A. Stephanovich, Phys. Rev. B **67**, 195203 (2003).

[15] T. L. Cocker, V. Jelic, M. Gupta, S. J. Molesky, J. A. J. Burgess, G. De Los Reyes, L. V. Titova, Y. Y. Tsui, M. R. Freeman, and F. A. Hegmann, Nat. Photon. **7**, 620 (2013); T. L. Cocker, D. Peller, P. Yu, J. Repp, and R. Huber, Nature (London) **539**, 263 (2016); L. Patera, F. Queck, P. Scheuerer, and J. Repp, *ibid.* **566**, 245 (2019).

[16] T. Kampfrath, K. Tanaka, and K. A. Nelson, Nat. Photon. **7**, 680 (2013).

[17] A. Kirilyuk, A. V. Kimel, and T. Rasing, Rev. Mod. Phys. **82**, 2731 (2010).

[18] T. Seifert, S. Jaiswal, J. Barker, S. T. Weber, I. Razdolski, J. Cramer, O. Gueckstock, S. Maehrlein, L. Nadvornik, S. Watanabe, C. Ciccarelli, A. Melnikov, G. Jakob, M. Münzenberg, S. T. B. Goennenwein, G. Woltersdorf, B. Rethfeld, P. W. Brouwer, M. Wolf, M. Kläui, and T. Kampfrath, Nat. Commun. **9**, 2899 (2018); S. Kovalev, Z. Wang,

J.-C. Deinert, N. Awari, M. Chen, B. Green, S. Germanskiy, T. V. A. G. de Oliveira, J. S. Lee, A. Deac, D. Turchinovich, N. Stojanovic, S. Eisebitt, I. Radu, S. Bonetti, T. Kampfrath, and M. Gensch, J. Phys. D **51**, 114007 (2018).

[19] V. A. Stephanovich and E. Ya. Sherman, Phys. Chem. Chem. Phys. **20**, 7836 (2018).

[20] V. A. Stephanovich, E. Ya. Sherman, N. T. Zinner, and O. V. Marchukov, Phys. Rev. B **97**, 205407 (2018).

[21] H. Imamura, P. Bruno, and Y. Utsumi, Phys. Rev. B **69**, 121303(R) (2004).

[22] K. Tao, V. S. Stepanyuk, W. Hergert, I. Rungger, S. Sanvito, and P. Bruno, Phys. Rev. Lett. **103**, 057202 (2009).

[23] S. Eich, M. Plötzing, M. Rollinger, S. Emmerich, R. Adam, C. Chen, H. C. Kapteyn, M. M. Murnane, L. Plucinski, D. Steil, B. Stadtmüller, M. Cinchetti, M. Aeschlimann, C. M. Schneider, and S. Mathias, Sci. Adv. **3**, e1602094 (2017).

[24] S. Loth, M. Etzkorn, C. P. Lutz, D. M. Eigler, and A. J. Heinrich, Science **329**, 1628 (2010); I. G. Rau, S. Baumann, S. Rusponi, F. Donati, S. Stepanow, L. Gragnaniello, J. Dreiser, C. Piamonteze, F. Nolting, S. Gangopadhyay, O. R. Albertini, R. M. Macfarlane, C. P. Lutz, B. A. Jones, P. Gambardella, A. J. Heinrich, and H. Brune, *ibid.* **344**, 988 (2014); S. Baumann, W. Paul, T. Choi, C. P. Lutz, A. Ardavan, and A. J. Heinrich, *ibid.* **350**, 417 (2015).

[25] M. Schüler, Y. Pavlyukh, and J. Berakdar, New J. Phys. **14**, 043027 (2012).

[26] I. Žutić, J. Fabian, and S. Das Sarma, Rev. Mod. Phys. **76**, 323 (2004).

[27] *Spin Physics in Semiconductors Springer Series in Solid-State Sciences,* edited by M. I. Dyakonov (Springer, Dordrecht, 2008).

[28] A. A. High, A. T. Hammack, J. R. Leonard, S. Yang, L. V. Butov, T. Ostatnický, M. Vladimirova, A. V. Kavokin, T. C. H. Liew, K. L. Campman, and A. C. Gossard, Phys. Rev. Lett. **110**, 246403 (2013).

[29] D. V. Vishnevsky, H. Flayac, A. V. Nalitov, D. D. Solnyshkov, N. A. Gippius, and G. Malpuech, Phys. Rev. Lett. **110**, 246404 (2013).

[30] E. I. Rashba and E. Ya. Sherman, Phys. Lett. A **129**, 175 (1988).

[31] H. Zhu, Y. Fu, F. Meng, X. Wu, Z. Gong, Q. Ding, M. V. Gustafsson, M. T. Trinh, S. Jin, and X. Y. Zhu, Nat. Mater. **14**, 636 (2015).

[32] Y. Rikitake and H. Imamura, Phys. Rev. B **72**, 033308 (2005)

[33] M. Isarov, L. Z. Tan, M. I. Bodnarchuk, M. V. Kovalenko, A. M. Rappe, and E. Lifshitz, Nano Lett. **17**, 5020 (2017).

[34] J. Even, L. Pedesseau, J.-M. Jancu, and C. Katan, J. Phys. Chem. Lett. **4**, 2999 (2013).

[35] F. Zheng, L. Z. Tan, S. Liu, and A. M. Rappe, Nano Lett. **15**, 7794 (2015).

[36] W. S. Yang, J. H. Noh, N. J. Jeon, Y. C. Kim, S. Ryu, J. Seo, and S. I. Seok, Science **348**, 1234 (2015).

[37] M. Saliba, S. Orlandi, T. Matsui, S. Aghazada, M. Cavazzini, J.-P. Correa-Baena, P. Gao, R. Scopelliti, E. Mosconi, K.-H. Dahmen, F. De Angelis, A. Abate, A. Hagfeldt, G. Pozzi, M. Graetzel, and M. K. Nazeeruddin, Nat. Energy **1**, 15017 (2016).

[38] S. D. Stranks and H. J. Snaith, Nat. Nanotechnol. **10**, 391 (2015).

[39] M. V. Costache, M. Sladkov, S. M. Watts, C. H. van der Wal, and B. J. van Wees, Phys. Rev. Lett. **97**, 216603 (2006).

[40] M. Battiato, K. Carva, and P. M. Oppeneer, Phys. Rev. Lett. **105**, 027203 (2010).

[41] S. Wienholdt, D. Hinzke, and U. Nowak, Phys. Rev. Lett. **108**, 247207 (2012).

[42] M. Kim, J. Im, A. J. Freeman, J. Ihm, and H. Jin, Proc. Natl. Acad. Sci. (USA) **111**, 6900 (2014).

[43] P. Yan, G. E. W. Bauer, and H. Zhang, Phys. Rev. B **95**, 024417 (2017); K. I. Uchida, H. Adachi, T. Kikkawa, A. Kirihara, M. Ishida, S. Yorozu, S. Maekawa, and E. Saitoh, Proc. IEEE **104**, 1946 (2016); E. J. Guo, J. Cramer, A. Kehlberger, C. A. Ferguson, D. A. MacLaren, G. Jakob, and M. Kläui, Phys. Rev. X **6**, 031012 (2016); M. Schreier, F. Kramer, H. Huebl, S. Geprägs, R. Gross, S. T. B. Goennenwein, T. Noack, T. Langner, A. A. Serga, B. Hillebrands, and V. I. Vasyuchka, Phys. Rev. B **93**, 224430 (2016); V. Basso, E. Ferraro, A. Magni, A. Sola, M. Kuepferling, and M. Pasquale, *ibid.* **93**, 184421 (2016); S. R. Etesami, L. Chotorlishvili, A. Sukhov, and J. Berakdar, *ibid.* **90**, 014410 (2014); U. Ritzmann, D. Hinzke, A. Kehlberger, E. J. Guo, M. Kläui, and U. Nowak, *ibid.* **92**, 174411 (2015); L. Chotorlishvili, X.-G. Wang, Z. Toklikishvili, and J. Berakdar, *ibid.* **97**, 144409 (2018); L. Chotorlishvili, Z. Toklikishvili, X.-G. Wang, V. K. Dugaev, J. Barnaś, and J. Berakdar, *ibid.* **99**, 024410 (2019); X. G. Wang, L. Chotorlishvili, G. H. Guo, and J. Berakdar, Phys. Lett. A **382**, 1100 (2018); J. Appl. Phys. **124**, 073903 (2018).

[44] V. A. Stephanovich, V. K. Dugaev, V. I. Litvinov, and J. Berakdar, Phys. Rev. B **95**, 045307 (2017).

[45] M. Pletyukhov and V. Gritsev, Phys. Rev. B **74**, 045307 (2006).

[46] S. M. Badalyan, A. Matos-Abiague, G. Vignale, and J. Fabian, Phys. Rev. B **79**, 205305 (2009).

[47] S. M. Badalyan, A. Matos-Abiague, G. Vignale, and J. Fabian, Phys. Rev. B **81**, 205314 (2010).

[48] E. M. Lifshitz and L. P. Pitaevskii, *Statistical Physics* (Pergamon, Oxford, 1980), Pt. 2.

[49] *Handbook of Mathematical Functions*, edited by M. Abramowitz and I. A. Stegun, National Bureau of Standards Applied Mathematics Series, Vol. 55 (National Bureau of Standards, Washington, DC, 1964).

[50] A. Abragam, *Principles of Nuclear Magnetism* (Oxford University Press, Oxford, 2006).

[51] V. I. Litvinov and V. K. Dugaev, Phys. Rev. B **58**, 3584 (1998).

[52] B. Fisher and M. W. Klein, Phys. Rev. B **11**, 2025 (1975).

[53] M. T. Beal-Monod, Phys. Rev. B **36**, 8835 (1987).

[54] M. Shiranzaei, J. Fransson, H. Cheraghchi, and F. Parhizgar, Phys. Rev. B **97**, 180402(R) (2018).

[55] D. L. Sounas and A. Alù, Phys. Rev. B **97**, 115431 (2018).

[56] J. Fransson, Phys. Rev. B **82**, 180411(R) (2010).

[57] S. R. Power, F. S. M. Guimarães, A. T. Costa, R. B. Muniz, and M. S. Ferreira, Phys. Rev. B **85**, 195411 (2012).

[58] X. Duan, V. A. Stephanovich, Y. G. Semenov, and K. W. Kim, Appl. Phys. Lett. **101**, 013103 (2012).

[59] G. Malinowski, F. D. Longa, J. H. H. Rietjens, P. V. Paluskar, R. Huijink, and H. J. M. Swagten, Nat. Phys. **4**, 855 (2008).